

HiSST: 4th International Conference on High-Speed Vehicle Science Technology 22 -26 September 2025, Tours, France



Carbon Fibre-Reinforced Polymer Laminates with Film Cooling: Thermo-Mechanical Performance under Moderate Heat Flux

Trista Yuting Ma¹, Nam Kyeun Kim², Priyanka Dhopade³, Tom Allen⁴

Abstract

Though carbon fibre-reinforced polymer (CFRP) composites have been extensively researched and used as structural components in aerospace applications, their relatively low thermal resistance has limited their adoption in high-speed vehicles. Integrating film cooling with CFRP structures has the potential to decrease thermal degradation, extending their use towards moderate heat flux zones in high-speed vehicles and pushing working temperatures beyond the conventional capabilities of CFRPs. However, no studies have been conducted to date on the coupled mechanical and thermal behaviour of film-cooled CFRPs under high temperatures, particularly over 500°C. This study investigates the mechanical degradation of film-cooled CFRP laminates having diameter, smaller than 1 mm perforations, as well as quantifying their thermal response. The laminate is exposed to steady-state heat flux ranging from 11.6 kW/m² to 30 kW/m² for 255 seconds to obtain its film cooling effectiveness using eight type-K thermocouples. Preliminary experimental results indicate a surface temperature reduction up to 55% on a 3mm-thick CFRP laminate. A hole-diameter-to-thickness (d/t) ratio of equal to 0.1, corresponding to a hole diameter of 0.3mm demonstrated no reduction in tensile and compressive strength.

Keywords: Film Cooling, Carbon Fibre-Reinforced Polymer (CFRP), Thermal Protection System, Open-hole Structural Degradation

1. Introduction

Carbon Fibre-Reinforced Polymers (CFRPs) have received rapidly increasing interests in aerospace and other high-performance industries due to their exceptional specific strength and stiffness, low density, low coefficient of thermal expansion and high corrosion resistance. Their application, however, has been limited to the matrix degradation temperature. Extending the operational range of CFRP components to high-temperature applications for the weight-sensitive parts is of interest, such as in hypersonic vehicles or the non-critical part on the thermal protection system in a reusable launch vehicle (RLV) has been the interest of recent research.

Film cooling has been extensively researched since the 20th century; recent advancement and development are reviewed in [1], [2], [3]. Compared to transpiration and convection cooling, film cooling achieves a balance of structural integrity, manufacture easiness and adequate thermal management. Transpiration cooling requires uniform porous structure, which is complex to manufacture, causing more uncontrolled variables. Contrarily, film cooling provides a continuous protective layer over the external surface, making it well-suited for broader areas of a component that require protection from a hot freestream. Its ability to create a thermal barrier with minimal structural and material modification makes it a suitable choice for a proof-of-concept study on CFRP laminates. Thus, active cooling, particularly, film-cooling was combined with CFRP laminates in this research.

¹ University of Auckland, New Zealand, trista.ma@auckland.ac.nz

² University of Auckland, New Zealand, nam.kim@auckland.ac.nz

³ University of Auckland, New Zealand, priyanka.dhopade@auckland.ac.nz

⁴ University of Auckland, New Zealand, tom.allen@auckland.ac.nz

Measurements and simulations by Ecker et al. reported heat fluxes of $<30~kW/m^2$ on base plates and $<100~kW/m^2$ on side walls at around 60km altitude for a supersonic rocket retro-propulsion maneuver [4]. Thus, a heat flux range of $11.3 \sim 30~kW/m^2$ was chosen to investigate the feasibility of film-cooled CFRP laminates. The thermal and mechanical performance of film-cooled CFRP laminates under the moderate heat flux condition were separately measured.

The paper is divided into two primary sections. First, a mechanical analysis is presented, evaluating the tensile and compressive strength of perforated CFRP laminates to quantify the strength reduction due to the introduced holes. Second, the film-cooling effectiveness of these laminates is assessed, focusing on how different hole sizes impact thermal performance. The latter part of this research is preliminary, with a discussion of the current experimental limitations provided at the end of the paper to guide future research.

2. Methodology

2.1. Specimen Manufacturing and Characterisation

The chosen pre-impregnated system, manufactured by Hankuk Carbon Co. Ltd., is composed of BH3T resin formulation, a high-temperature epoxy-based matrix, and M40JB high-modulus carbon fibre with a fibre volume fraction of 0.6 [5]. The prepreg is supplied as a unidirectional (UD) tape, 300 mm in width, with a specific weight of 300 gsm. The lay-up sequence chosen was [0, 90, -45, 45, 90, 0, 90, 45, -45, 90, 0], in line with previous work on rocket primary structures [6]. Laminates were fabricated at the University of Auckland, following the curing cycle supplied by Hankuk: first, the oven temperature increased from 20°C to 80°C at a constant rate of 1-3 °C/min with an initial dwell of 1 hour at 80 °C, followed by a second temperature ramp from 80°C to 135°C, at 1-3 °C/min, with a second dwell of 1.5 hours at 135 °C. The laminates were cooled down naturally to room temperature. The resulting nominal thickness was in the range of $3.2 \pm 0.17 mm$.

Specimens for tensile and combined loading compression (CLC) tests were prepared according to ASTM D3039 and ASTM D6641, respectively. The specimens had a nominal length of 140 mm and a width of 18~20mm. This length was chosen to minimise material usage and reduce manufacturing time while ensuring that failure occurred within the gauge section, independent of grip-induced stress concentrations.

The specimen coupons and the central cutout were precisely prepared using a Computer Numerical Control (CNC) machine. A SECO dura coated solid carbide 4 flute composite was used for cutting of the specimens. Cutting was performed at a spindle speed of 4000 RPM and a feed rate of 2000 mm/min, while drilling holes used 6000 RPM at a feed rate of 50 mm/min. To ensure the composite laminate was firmly secured and to prevent any movement or vibration during the cutting process, it was affixed to a solid aluminium block using double-sided tape with vacuum-assistance. After the initial cutting, each specimen was carefully removed. The ends of the specimens were then machined in parallel to ensure a uniform and consistent load transfer during the compression tests, following the ASTM D6641 standard. The hole(s) were drilled after the parallelizing process to maintain their precise central location relative to the newly machined specimen ends.

2.2. Mechanical Testing

Both the tensile and CLC tests were conducted using an Instron 1185 universal testing machine equipped with a 100 kN load cell. The tests were performed under controlled environmental conditions, specifically at a temperature of 20 ± 2 °C and relative humidity of 60 ± 5 %.

Tensile Strength Test

For tensile testing, a clip-on extensometer of INSTRON 2630-123 with an accuracy of $\pm 1.5 \mu m$ was used for the specimens that do not have holes through. Spacers were used in the tensile test jig to ensure the loading acts through the centre of the specimen, thus no moment was generated in the specimens. The crosshead speed was set to at 2 mm/min according to ASTM D3039/D3039M with a sampling frequency of 20Hz.

Compressive Strength Test

According to ASTM D6641/D6641M, two strain gauges were mounted back-to-back on the centre of the no-hole specimens to measure strain on both faces. The difference in strain values between the two gauges was under a threshold of 10%, which confirmed that a uniaxial compressive load was being applied. For the holed specimens, bending was not considered a significant issue because the pre-existing stress concentration at the hole's edge would lead to failure before any critical bending-induced failure could occur. The strain gauge was not required based on the primary interest of the study is to measure the reduction of compressive strength and determine the failure strain. The crosshead speed was set at 1.3 mm/min. Data were recorded using the machine's integrated data acquisition system at a sampling rate of 20 Hz.

2.3. In-Situ Digital Image Correlation (DIC) Methodology

To provide a full-field analysis of strain distribution and to validate the failure modes observed with the

high-speed camera, a 2D DIC setup was employed (Figure 1). The system consisted of a high-resolution camera, and the specimens were illuminated by two LED spotlights to ensure consistent lighting throughout the tests. A random, high-contrast speckle pattern was applied to the gauge section of each specimen using spray paint. Images were captured at a rate of 2Hz throughout the tensile test until failure. The acquired images were analysed using NCorr in MATLAB.

A parametric study was conducted the subset radius to optimise the balance between the precision (low noise) and spatial resolution (ability to capture sharp strain gradients) across the hole, where peak strain occurs. All other analysis parameters were held constant. A correlation-cutoff coefficient of 0 means no match while 1 means a perfect match. A cutoff of 0.8 is commonly used, thus chosen for this analysis as it excludes unreliable data but allows acceptable errors from an experimental setup.



Figure 1 DIC Setup

Figure 2 shows that the smallest subset radius of 10 generated a great amount of noise. The study found that a subset radius of 30 with a subset spacing of 3 was sufficient to capture the peak strain values while minimising noise. A radius of 25 showed similar noise levels, but its peak strain value at the stress concentration was lower, indicating that it was smearing the strain and underestimating the true peak.

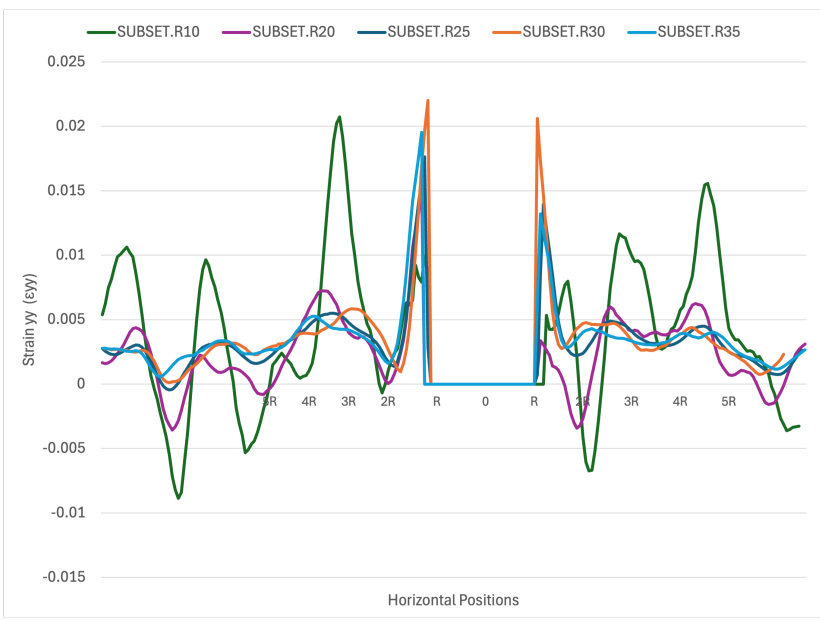


Figure 2 Parametric Study on Subset Size

3. Results and Discussions

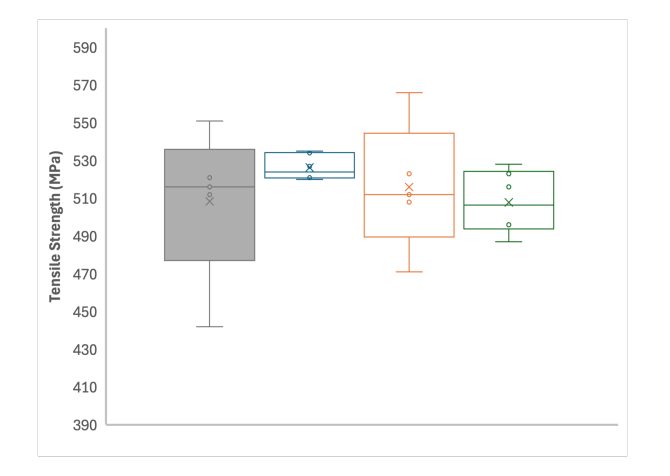
3.1. Tensile Test

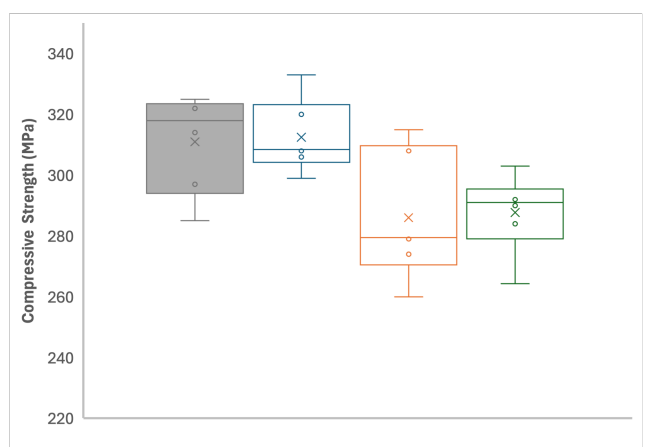
This study investigated four sample groups to assess the effect of small perforations on tensile strength: No holes (control group), a single 2 mm circular hole (2 mm \times 1 hole), two perforations with a diameter of 1 mm (1 mm \times 2 holes) and three perforations with a diameter 0.6 mm (0.6 mm \times 3 holes). The ultimate tensile strength for each group was determined and is presented in Table 1 with 3 significant figures.

Table 1 Change in Tensile Strength for Different Groups

Group	Mean Tensile	Standard	∆ in Mean Value	p-value	
	Strength (MPa)	Deviation (MPa)	to no hole group		
No hole, width 20mm	508	40.2	-	-	
0.6 mm x 3 holes	526	6.80	+ 3.50 %	0.932	
1 mm x 2 holes	516	34.1	+ 1.50 %	0.755	
2 mm x 1 hole	508	16.7	- 0.100 %	0.914	

The experimental results show that all perforated groups experienced no statistically significant reduction in tensile strength compared to the unperforated control group, as all the p-values are significantly greater than 0.05, shown in Table 1 . This is a notable deviation from expected behaviour based on previous literature, which however, is primarily focused on larger-diameter perforations. Intriguingly, the 0.6 mm holes exhibited a normalised strength greater than 1, suggesting a slight increase in ultimate tensile strength. This counter-intuitive finding can be attributed to several factors. First, the result falls within the statistical scatter inherent in composite material testing as shown in Figure 3a; the variance within the controlled group is much larger than the 0.6 mm holes group.





■ No holes, 13mm □ 0.6 mm x 3 holes □ 1 mm x 2 holes □ 2mm x 1 hole

Figure 3 Hole Size Effects on Mechanical Strength (a)Tensile Strength (b)Compressive Strength

The DIC analysis presented the strain distribution and failure mechanisms of the perforated laminates. For all perforated groups, the DIC maps clearly showed strain concentrations at the hole boundaries. A quantitative analysis of the strain concentration factor $(K\epsilon)$ was performed on the 0.6 mm, 1 mm, and 2 mm hole groups at a load corresponding to 80% of the specimen's ultimate strength. This loading provides representative data for strain concentration effects without the confounding factors of final fracture. The appropriate DIC frames were selected by synchronizing the image capture time with the force measurement data from the INSTRON machine. The strain concentration factor $(K\epsilon)$ was calculated by plotting a line of strain across the face of the specimen, passing through the centre of the hole(s). The peak strain value, located just outside the hole's boundary was then divided by the

HiSST-2025 4 far-field strain value, located at 20 mm away from the centre of the hole(s) from the same image. Table 1 summarized the strain concentration factor.

The strain fields showed no interaction between adjacent holes as the hole-to-diameter (p/d) ratio was kept consistently at 10 for all groups as shown in Figure 4. The noise in Figure 5 is attributed to the relatively large speckle patterns used, which did not undergo significant deformation in the longitudinal direction, making small strain ϵ_{vv} measurements sensitive to minor pattern imperfections.

For the 2 mm hole, the strain maps showed a clear zone of maximum strain initiation that corresponded precisely to the crack path observed in a high-speed camera, traveling from the hole to the grip section (Figure 6). For holes that are smaller than 2 mm, the DIC maps also highlighted the zones of failure initiation, even if the rapid micro-scale failure was difficult to pinpoint with the high-speed camera alone. These DIC results provide strong visual evidence that although the perforations did not significantly reduce the ultimate tensile strength, they fundamentally altered the stress and strain state of the laminate.

Table 2 Strain Concentration Factor from Notched Group

Notched Group	Strain Concentration Factor $K\epsilon$
0.6 mm x 3 holes	3.2
1 mm x 2 holes	4.2
2 mm x 1 hole	12

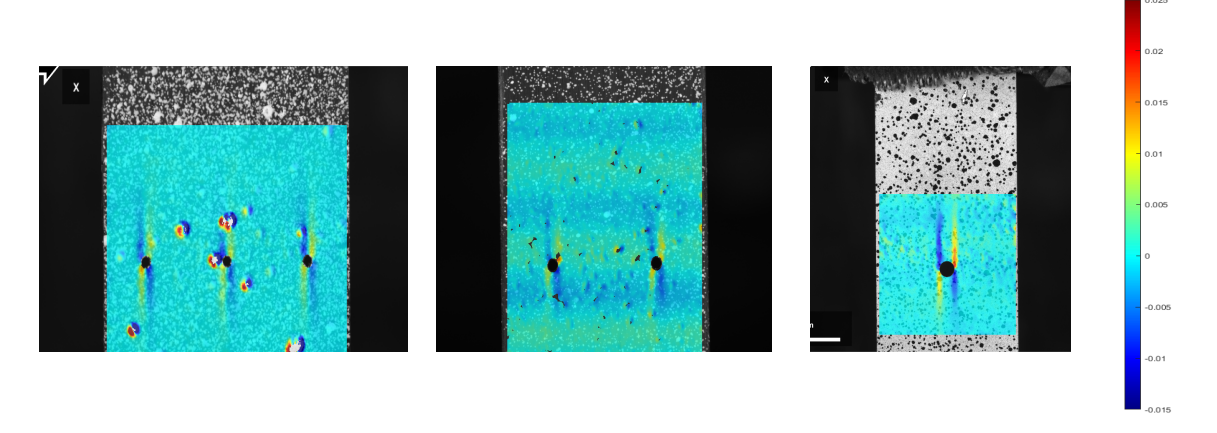
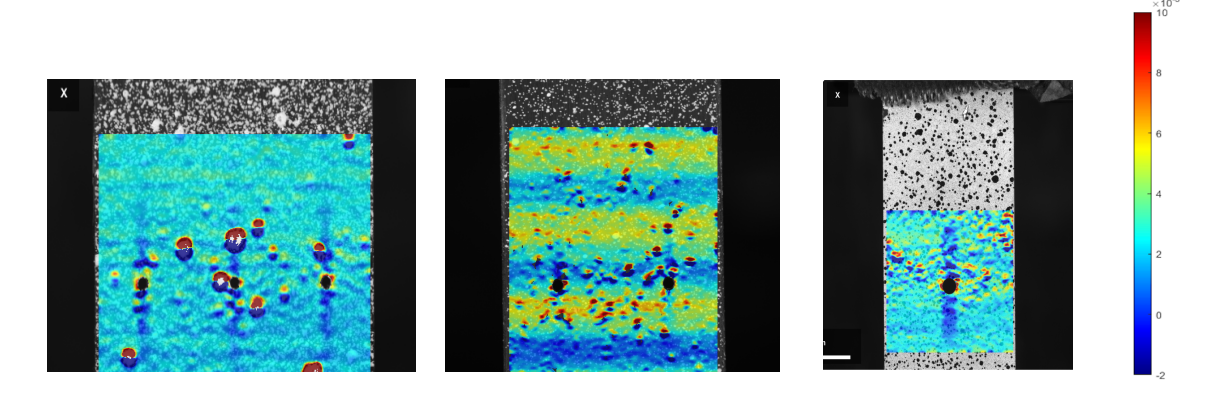


Figure 4 DIC Images of Shear Strain, ϵ_{xy} (a) 0.6 mm holes (b) 1 mm holes (c) 2 mm hole



HiSST-2025 Page |

5

Figure 5 DIC Images of Longitudinal Strain, ϵ_{yy} (a) 0.6 mm holes (b) 1 mm holes (c) 2 mm hole

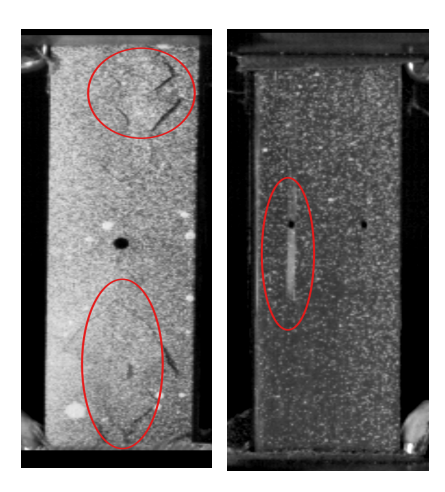


Figure 6 High-speed Camera Captured Failure

3.2. Combined Loading Compressive (CLC) Test

The experimental results showed no statistically significant difference in compressive strength compared to the no hole group, except for the 1 mm holes. As very few studies have investigated the compressive behaviour of CFRP with such small cutouts, no reduction could suggest a critical threshold exists below which the localised stress concentration caused by a cutout is negligible that it does not initiate the complex failure mechanisms (like fibre buckling or kinking), which would degrade the material's overall compressive strength. More visual analysis is needed to investigate the interaction between the micro and macro-level failure.

Despite a consistent cutout percentage of 10%, a clear difference in compressive strength was observed based on absolute hole diameter. The 1 mm and 2 mm hole groups experienced a statistically significant reduction in strength compared to the 0.6 mm group, as indicated by a p-value of less than 0.05 when analysed against the 0.6 mm holes group. Specifically, a 7.5% and 8.5% strength reduction was measured for the 2 mm and 1 mm groups, respectively, relative to the 0.6 mm group.

The unexpectedly large variance and greater-than-expected strength reduction observed in the 1 mm hole group suggest that the relationship between hole size and compressive strength is not purely linear at this scale. Potential contributing factors for this variation include differences in the drilling process, as the specimens for the 1 mm group were cut from a separate panel, or microstructural variations within the laminates themselves. This result highlights that for compressive strength, the impact of a perforation is not solely a function of cutout percentage but may also dependent on the absolute hole diameter.

The effect of the specimen width-to-hole diameter ratio (w/d) on compressive strength was investigated using the 2 mm-hole group. Specimens with widths of 18 mm (w/d=9) and 20 mm (w/d=10) were tested. The mean average compressive strength for these two groups was found to be statistically identical. This result is in strong agreement with established literature, which indicates that for w/d ratios greater than approximately 6, the stress concentration effect of the hole becomes localised and the overall strength becomes independent of the specimen width [7]. In such cases, the stress field around the hole is contained well within the specimen, and the far-field stress state is representative of the true open-hole condition. The compressive strength plots for both the 18 mm and 20 mm widths clearly overlap, visually confirming that the specimens were sufficiently wide to avoid specimen-edge effects and to exhibit the true open-hole compressive strength of the material. This demonstrates that the chosen specimen geometry effectively isolated the hole-size effect without being influenced by w/d, which is considered as a critical parameter in the open-hole tensile and compressive tests.

Table 3 Change in Compressive Strength for Different Groups

Group	Mean Compressive Strength (MPa)	Standard Deviation (MPa)	Δ in Mean Value to no hole group	p- value
No hole	311	16.4	-	-
0.6 mm x 3 holes	313	12.1	+ 0.482%	0.860
1 mm x 2 holes	286	21.1	- 8.04 %	0.045
2 mm x 1 hole, width 20mm	288	15.6	- 7.52%	0.078

4. Film Cooling Performance

To evaluate the cooling effectiveness based on the different hole sizes, a film cooling experiment was conducted under steady-state heat flux conditions. The experimental setup employed water as the coolant, selected for its high specific heat capacity, widespread availability, and proven effectiveness in recent active-cooling research, providing a robust proof-of-concept.

4.1. Film-cooling Experimental Methodology

The panel geometry measured 150 mm by 150 mm, with a central 100 mm by 100 mm region subjected to a quasi-uniform, steady-state heat flux. Two groups of specimens were tested, each with a different hole size to investigate the effect of perforation diameter on cooling effectiveness:

- Group 1: 1 mm holes, cut using a CNC machine.
- Group 2: 0.3 mm holes, cut using a femto-second laser.

The pitch distance (the center-to-center distance between adjacent holes) was maintained at a constant ratio of 10 (i.e. P/D=10). A total coolant flow rate of 185 ccm (cubic centimeters per minute) was delivered via a pump. The heat source consisted of four ceramic heaters, placed 70 mm from the panel surface. This setup generated a constant heat flux of 11.3 kW/m², 25.6 kW/m² and 29.1 kW/m², based on the temperature setting of the heaters of 500°C, 750°C and 800°C, respectively. The heat flux was calibrated and monitored using a water-cooled heat flux sensor. The total test duration was 255 s, a period determined from preliminary calibration tests that showed the panel's temperature stabilised after approximately 120 s, indicating steady-state conditions had been reached. The temperature was calculated by averaging three sets of data, from the final minute of the test (from 180s to 255s), ensuring all values were taken from the steady-state period with statistical confidence. The resulting temperatures are summarised in Table 4 below.

Table 4 Film Cooling Effectiveness by Hole Group and Heat Flux

Heat Source Temperature (°C)	Hole Group	TC1 (°C)	TC2 (°C)	TC3 (°C)	TC4 (°C)	TC5 (°C)	TC6 (°C)	TC7 (°C)	TC8 (°C)
500°C	1 mm (number of holes?)	45.6	42.1	45.3	85.5	53.5	44.3	45.6	45.6
	0.3 mm (number of holes?)	33.5	25.5	33.4	35.0	33.3	35.9	30.8	35.3
% difference		-27%	-39%	-26%	-59%	-38%	-19%	-6%	-23%
750°C	1 mm	95.6	61.9	64.6	98.8	66.3	-	47.2	82.8
	0.3 mm	53.3	33.0	49.5	58.1	53.5	59.6	45.6	53.9
% difference		-44%	-47%	-23%	-41%	-19%	-	-4%	-35%
800°C	1 mm	104.8	80.2	81.5	145.7	103.5	-	54.5	100.7
	0.3 mm	57.2	36.0	53.9	64.9	60.8	71.4	48.6	59.1
% difference		-45%	-55%	-34%	-55%	-41%	-	-11%	-41%

4.2. Film Cooling Results

The experimental results demonstrate a clear and significant temperature reduction on the surface of the CFRP laminates due to the film-cooling effect. Overall, a temperature reduction ranging from 26% to 60% was found, compared to a panel without cooling. The degree of cooling is highly dependent on the measurement location and the applied heat flux level.

The thermal performance of the panel was monitored using eight Type-K thermocouples, shown in Figure 7. To demonstrate the representative nature of the data, the temperature measurements from only three thermocouples are presented in Figure 8. This is because thermocouples TC4, TC5, and TC6 were positioned directly behind TC1, TC2, and TC3 respectively, and consistently followed the same temperature trends.

HiSST-2025 8 Ma. T, Kim. N, Dhopade. P, Allen. T

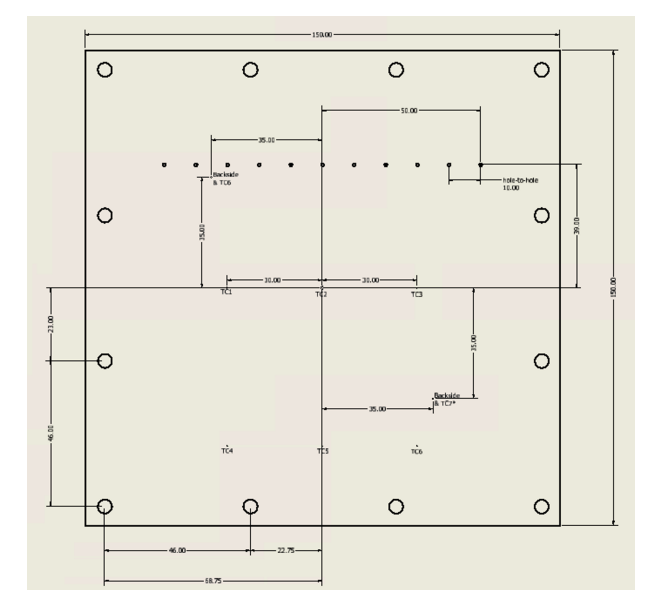


Figure 7 Thermocouple Positions

It is evident from the temperature measurements that the 0.3 mm hole group provided superior cooling performance compared to the 1 mm group, despite operating at the same total flow rate. This outcome is primarily attributed to the smaller holes' ability to provide a more uniform and contiguous film of coolant over the panel's surface. With a greater number of smaller holes, the coolant is distributed more evenly, resulting in better film coverage and a more effective thermal barrier against the high heat flux.

Other factors may also contribute to this difference. The manufacturing method, specifically femtosecond laser cutting for the 0.3 mm holes versus CNC drilling for the 1 mm holes, could have resulted in cleaner hole geometry and smoother internal surfaces. These factors can lead to less turbulent flow and better adherence of the coolant jet to the surface, which is critical for film-cooling efficiency. It is worth noting that a flow rate higher than the current setup caused the coolant to detach from the surface, a phenomenon known as jet lift-off, which would adversely impact cooling effectiveness.

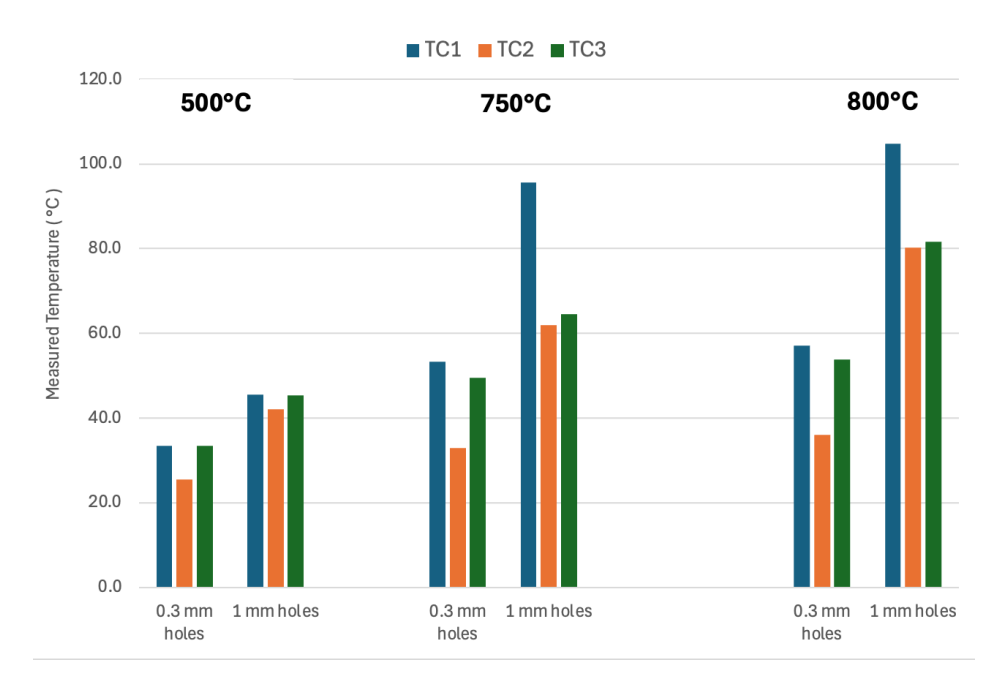


Figure 8 Thermocouple Data Under Different Heat Flux

4.3. Experimental Limitations and Future Work

This preliminary study provides valuable insights into the film cooling of perforated CFRPs but is subject to several key limitations that should be addressed in future work.

The current experimental setup lacks a freestream flow, which is a significant departure from real-world applications. A hot freestream flow would introduce complex turbulent mixing with the coolant jets, which would likely cause the jets to lift off and dilute more rapidly, reducing the cooling effectiveness downstream. This would require the adjustment on the flow rate to achieve a desired blowing ratio to keep the flow attached to the surface, as jet lift-off effect have been extensively concluded to adversely impact the cooling effect. Future work should incorporate a wind tunnel or similar setup to simulate a freestream flow and investigate its impact on the measured cooling effectiveness.

Furthermore, the use of a limited number of thermocouples provides only localized temperature measurements. A more comprehensive understanding of the cooling performance requires a full-field temperature map. This can be achieved using an IR camera, which would provide a global view of the temperature distribution and identify areas of low and high cooling effectiveness. This would also help to visualise the film's spread and coverage, helping to find the optimal hole size.

Additionally, the observations from the 1 mm hole group suggest that the pitch distance of 10 was not desirable, as the individual coolant jets do not coalesce to form a continuous film. Future work should investigate a parametric study with a reduced pitch-to-diameter ratio to determine the optimal spacing for a continuous film. Alternatively, a design with multiple rows of holes could be investigated to see if adding more jets in a staggered array could create a more effective film.

5. Conclusion

This study investigated separately the thermal and mechanical performance of perforated CFRP laminates with film cooling as a starting point for future research. The mechanical tests showed that small perforations did not reduce the laminates' ultimate tensile strength, with minimal reduction in the compressive strength, despite the presence of stress concentrations at the hole boundaries.

Film cooling experiments with water demonstrated significant temperature reductions. The 0.3 mm holes provided superior surface coverage compared to the 1 mm holes, suggesting that a greater number of smaller jets form a more effective protective film but would require greater pump pressure.

The primary limitation of this research was the absence of a hot freestream flow. Future work should incorporate a freestream flow and the use an infra-red camera to obtain a full-field temperature map. A parametric study on the pitch-to-diameter ratio for larger holes is necessary to find the balance between cooling effectiveness and strength reduction.

References

- [1] S. Acharya and Y. Kanani, "Chapter Three Advances in Film Cooling Heat Transfer," in *Advances in Heat Transfer*, vol. 49, E. M. Sparrow, J. P. Abraham, and J. M. Gorman, Eds., Elsevier, 2017, pp. 91–156. doi: 10.1016/bs.aiht.2017.10.001.
- [2] FEDERICO GIAMBELLI, RICCARDO BISIN, ENRICO BRAGALLI, and CHRISTIAN PARAVAN, "Liquid Film Cooling: Open-Literature Review, Modeling and Efforts Towards Validation," p. 23 pages, 2023, doi: 10.13009/EUCASS2023-648.
- [3] R. J. Goldstein, "Film Cooling," in *Advances in Heat Transfer*, vol. 7, T. F. Irvine and J. P. Hartnett, Eds., Elsevier, 1971, pp. 321–379. doi: 10.1016/S0065-2717(08)70020-0.
- [4] T. Ecker, S. Karl, E. Dumont, S. Stappert, and D. Krause, "Numerical Study on the Thermal Loads During a Supersonic Rocket Retropropulsion Maneuver," *J. Spacecr. Rockets*, vol. 57, no. 1, pp. 131–146, Oct. 2019.

- [5] Hankuk Carbon Co. Ltd., "B3ht datasheet." Sept. 23, 2020.
- [6] A. Blackwell, "Characterization of CFRP laminates under varied thermal environments for space applications," ResearchSpace@Auckland, 2024. Accessed: Apr. 15, 2025. [Online]. Available: https://hdl.handle.net/2292/70044
- [7] C. Soutis, "Compressive strength of composite laminates with an open hole: Effect of ply blocking," *J. Compos. Mater.*, vol. 47, no. 20–21, pp. 2503–2512, Sept. 2013, doi: 10.1177/0021998312466122.